HOKKAIDO UNIVERSITY

Title	Activation cross sections of 7Li-induced reactions on natCu for monitor reactions
Author(s)	Aikawa, Masayuki; Goto, Saki; Gantumur, Damdinsuren et al.
Citation	Nuclear Instruments and Methods in Physics Research Section B: Beam Interactions with Materials and Atoms, 554, 165441 https://doi.org/10.1016/j.nimb.2024.165441
Issue Date	2024-09
Doc URL	https://hdl.handle.net/2115/97200
Rights	©2024. This manuscript version is made available under the CC-BY-NC-ND 4.0 license https://creativecommons.org/licenses/by-nc-nd/4.0/
Rights(URL)	https://creativecommons.org/licenses/by-nc-nd/4.0/
Type	journal article
File Information	Nucl Instrum Methods Phys Res B_554.pdf

Hokkaido University Collection of Scholarly and Academic Papers : HUSCAP

Activation cross sections of ^{7}Li-induced reactions on ^{nat}Cu for monitor reactions

Masayuki Aikawa [a,b,c,*], Saki Goto [c], Damdinsuren Gantumur [c], Dagvadorj Ichinkhorloo [d], Naoyuki Ukon [e], Naohiko Otuka [f], Sándor Takács [g], Hiromitsu Haba [h]

[a] *Faculty of Science, Hokkaido University, Sapporo 060-0810, Japan*

[b] *Global Center for Biomedical Science and Engineering, Faculty of Medicine, Hokkaido University, Sapporo 060-8648, Japan*

[c] *Graduate School of Biomedical Science and Engineering, Hokkaido University, Sapporo 060-8638, Japan*

[d] *Nuclear Research Center, National University of Mongolia, Ulaanbaatar 13330, Mongolia*

[e] *Advanced Clinical Research Center, Fukushima Medical University, Fukushima 960-1295, Japan*

[f] *Nuclear Data Section, International Atomic Energy Agency, A-1400 Wien, Austria*

[g] *HUN-REN Institute for Nuclear Research, ATOMKI, Debrecen 4026, Hungary*

[h] *Nishina Center for Accelerator-Based Science, RIKEN, Wako 351-0198, Japan*

Abstract

Activation cross sections of ^{7}Li-induced reactions on ^{nat}Cu were measured in order to investigate suitability of some reactions for monitoring experimental parameters. Cross sections producing ^{69,68}Ge, ^{67,66}Ga and ^{69m,65}Zn were determined. Physical thick target yields were experimentally measured and compared with those calculated using the measured cross sections. The measured cross sections were verified by the agreements between the directly measured thick target yields and the thick target yields deduced from the measured cross sections. The ^{7}Li-induced reactions on ^{nat}Cu for the production of ^{67,66}Ga and ^{65}Zn are suggested as monitor reactions.

Keyword

^{7}Li induced reaction on ^{nat}Cu; Monitor reaction; Production cross section of ^{69,68}Ge, ^{67,66}Ga, and ^{69m,65}Zn; Excitation function

1. Introduction

Charged-particle-induced reactions are used for radionuclide production for different applications, such as imaging and therapy in nuclear medicine. One attractive radionuclide for nuclear medicine is ^{211}At, which has a half-life of 7.214 h and is promising radionuclide for targeted α-particle therapy [1–3]. Its longer-lived parent nucleus ^{211}Rn ($T_{1/2}$ = 14.6 h) can be employed in the ^{211}Rn/^{211}At generator [4,5]. One potential production route of the ^{211}Rn radionuclide is through ^{6}Li- and ^{7}Li-induced reactions on a ^{209}Bi target. In order to maximize the production of ^{211}Rn under the constraint to minimize the unnecessary by-products, monitor

* Corresponding author: Masayuki AIKAWA (aikawa@sci.hokudai.ac.jp), Faculty of Science, Hokkaido University, Sapporo 060-0810, Japan

reactions play an important role to determine and monitor the optimal beam parameters. As there are no established monitor reactions for both stable lithium isotopes, ^{6}Li and ^{7}Li, as projectiles, we started a systematic study to select target materials for possible monitor reactions.

Copper is a target material of monitor reactions for proton-, deuteron-, ^{3}He- and α-particle-induced reactions [6,7]. As a ^{7}Li beam is more frequently used than the beam of ^{6}Li we focused on ^{7}Li-induced reactions on ^{nat}Cu. In the literature survey based on the latest version of EXFOR library [8], only one experimental study was found below 100 MeV [9]. We performed experiments at the 72-MeV ^{7}Li energy to measure activation cross sections of the reactions in which longer-lived reaction products are formed. The reaction cross sections for formation of ^{69,68}Ge, ^{67,66}Ga, and ^{69m,65}Zn on ^{nat}Cu targets bombarded by ^{7}Li projectiles were determined. In order to verify the experimentally measured cross sections physical thick target yields were also determined experimentally and were compared with calculated ones based on the measured cross sections.

2. Experimental details and data analysis

We conducted three experiments; two experiments were dedicated for measurements of excitation functions and one for determination of thick target yields of selected reactions. Beams of ^{7}Li particles at 72 MeV were used for irradiation at the AVF cyclotron in RIKEN. The stacked-foil activation technique was applied. In order to identify the radioactive products γ-ray spectrometry was used in all experiments.

Three separate targets were prepared for the three experiments. Targets #1 and #2 served for excitation function measurements and were composed of thin metallic foils of ^{nat}Cu (5-μm thick, 99.9 % purity, Nilaco Corp., Japan), ^{nat}Ti (5-μm thick, 99.5 % purity, Nilaco Corp., Japan), and ^{27}Al (5-μm thick, >99 % purity, Nilaco Corp., Japan). The nominal sizes of original foils of ^{nat}Cu, ^{nat}Ti and ^{27}Al were 100 mm × 100 mm, 50 mm × 100 mm and 100 mm × 100 mm, respectively. The size and weight of each foil were measured to determine the average thickness. The obtained average thicknesses of ^{nat}Cu, ^{nat}Ti and ^{27}Al were 4.49 ± 0.04, 2.34 ± 0.02 and 1.21 ± 0.01 mg/cm^2, respectively. The foils were cut into a size of 8 mm × 8 mm to fit in the target holders that served also as a Faraday cup to collect the charge during irradiation. To shift the effective midpoint energy in the Cu foils the sequence of the foils in the two targets were modified. Both of the stacked targets were composed of 17 groups of the foils in the sequence of Cu-Al-Ti-Al for #1 and Ti-Al-Cu-Al foils for #2. The ^{27}Al foils were used to catch the recoiled reaction products from the ^{nat}Cu or ^{nat}Ti foils adjacent at the beam upstream. The target #3 prepared for the yield measurement consisted of 25-μm thick ^{nat}Cu foils. The average thickness determined from the measured size and weight of the original foil (100 mm × 100 mm, 99.9 % purity, Nilaco Corp., Japan) was 21.5 ± 0.2 mg/cm^2. The foil was cut into a size of 10 mm × 10 mm pieces and were stacked into another target holder. Only eight of the ^{nat}Cu foils were stacked in the target holder without any additional foil. The target information regarding the three targets is summarized in Table 1.

The stacked-foil targets #1, #2 and #3 were irradiated with ^{7}Li beams for 60, 60 and 30 min, respectively. The average beam currents determined using the irradiation period and the total charge collected by the

Faraday cup were 314 ± 16 (#1), 321 ± 16 (#2), and 309 ± 15 nA (#3). The beam energy was determined by the time-of-flight method [10]. Three subsequent irradiations were performed with the same cyclotron settings; therefore the 71.6 ± 0.4 MeV incident beam energy was common for the three experiments. Energy degradation of the bombarding particles in the targets was calculated layer by layer using stopping powers obtained from the SRIM code [11]. The beam parameters are also summarized in Table 1.

The emitted γ rays originated from the activated foils were measured using two high-purity germanium detectors of the same type (ORTEC GEM30P4-70). One of the detectors was used for γ-ray measurements for the experiment #1 and the other for the experiment #2. Both detectors were used in case of the experiment #3. Dedicated software (SEIKO EG&G Gamma Studio) was used for spectrum data analysis. The efficiency of the two detectors was calibrated using the same calibrated γ-ray sources, a multiple γ-ray source consisting of ^{57,60}Co, ^{85}Sr, ^{88}Y, ^{109}Cd, ^{113}Sn, ^{137}Cs, ^{139}Ce, ^{203}Hg and ^{241}Am (Eckert & Ziegler Isotope Products) and an ^{152}Eu source (Japan Radioisotope Association). For both of the calibrated γ-ray sources the diameter of the activity spot was similar to the diameter of the beam spot, therefore no additional geometry correction was necessary to apply. Each irradiated foil was measured four times to be able to follow the decay of the products with different half-lives. Cooling time varied between 9.49 h and 270.93 d. The associated dead time never exceeded 5.2 % due to adjusting the distance between the foils and detector surface. The detailed parameters of the measurements are listed in Table. 2. The nuclear data for the γ-ray spectrometry were retrieved from the online databases, NuDat 3.0 [12], LiveChart [13], and QCalc [14]. The retrieved data are summarized in Table 3.

Activation cross sections were deduced using the following equation

$$\sigma = \frac{N_{E_\gamma}\lambda}{\varepsilon_{E_\gamma} I_{E_\gamma} \varepsilon_t n_t n_b (1 - e^{-\lambda t_b}) e^{-\lambda t_c} (1 - e^{-\lambda t_m})} \quad (1)$$

where E_γ is the γ-ray energy, N_{E_γ} is the net count of the peak area, λ is the decay constant (s^{-1}), ε_{E_γ} is the detector efficiency, I_{E_γ} is the γ-ray intensity, ε_t is the dead time correction, n_t is the areal number density of target atoms (cm^{-2}), n_b is the number of projectiles per unit time (s^{-1}), t_b is the irradiation time (s), t_c is the cooling time (s), and t_m is the acquisition time (s).

Experimental and calculational physical thick target yields (Bq/C) [15] were deduced from the following equations

$$Y = \frac{\lambda}{Ze} \frac{N_{E_\gamma}\lambda}{\varepsilon_{E_\gamma} I_{E_\gamma} \varepsilon_t n_b (1 - e^{-\lambda t_b}) e^{-\lambda t_c} (1 - e^{-\lambda t_m})} \quad (2)$$

$$Y = \frac{\lambda}{Ze} \int_0^{E_{\text{in}}} \frac{\sigma(E)}{S(E)} dE \quad (3)$$

where Z is the atomic number of the projectile, e is the elementary charge (C), E_{in} is the incident energy of the projectile (MeV), $S(E)$ is the stopping power per areal number density of the target (MeV cm^2).

Table 1. Target and beam information.

	Exp. #1	Exp. #2	Exp. #3

Target			
Cu foil (mg/cm^2)	4.49 ± 0.04	4.49 ± 0.04	21.5 ± 0.2
Ti foil (mg/cm^2)	2.34 ± 0.02	2.34 ± 0.02	
Al foil (mg/cm^2)	1.21 ± 0.01	1.21 ± 0.01	
Configuration	17 sets of Cu-Al-Ti-Al foils	17 sets of Ti-Al-Cu-Al foils	8 Cu foils
Beam			
Energy (MeV)	71.6 ± 0.4	71.6 ± 0.4	71.6 ± 0.4
Average current (nA)*	314 ± 16	321 ± 16	309 ± 15
Irradiation period (min)	60	60	30

* Electric beam current in nA for the 3+ charge state of ^{7}Li beams.

Table 2. γ-ray measurement information (cooling time, distance, and dead time in each series).

Series	Exp. #1	Exp. #2	Exp. #3
1	1.4–3.0 h, 100 cm, 0.2–2.1 %	4.9–6.7 h, 100 cm, <0.9 %	33–35 h, 50–100 cm, 0.3–2.7 %
2	5.2–29 h, 50 cm, 0.3–1.3 %	24–34 h, 50 cm, <1.1 %	43–47 h, 50 cm, 0.2–5.2 %
3	3.7–4.1 d, 10 cm, 0.2–2.6 %	3.8–4.1 d, 10 cm, <2.3 %	59 d, 5 cm, 0.1–1.1 %
4	57–58 d, 5 cm, <0.1 %	58–59 d, 5 cm, <0.1 %	59 d, 5 cm, 0.1–1.1 %

Table 3. Reaction and decay data retrieved from online databases [12–14]. The γ lines in bold fonts were used for the analysis.

Nuclide	Half-life	Decay mode (%)	E_γ (keV)	I_γ (%)	Contributing reaction	Q-value (MeV)
^{69}Ge	39.05 h	ε+β^+ (100)	574.11	13.3 ± 1.8	^{65}Cu(^{7}Li,3n)	-9.5
			871.98	11.9 ± 1.6	^{63}Cu(^{7}Li,n)	8.4
			1106.77	**36 ± 4**		
^{68}Ge	270.93 d	ε (100)	-	-	^{65}Cu(^{7}Li,4n)	-17.7
					^{63}Cu(^{7}Li,2n)	0.2
^{68}Ga	67.71 min	ε+β^+ (100)	**1077.34**	**3.22 ± 0.03**		
^{67}Ga	3.2617 d	ε (100)	93.31	38.81 ± 0.03	^{65}Cu(^{7}Li,t2n)	-16.6
			184.58	21.410 ± 0.010	^{63}Cu(^{7}Li,t)	1.26
			300.22	**16.64 ± 0.12**	^{67}Ge decay	
^{66}Ga	9.49 h	ε+β^+ (100)	**1039.22**	**37.0 ± 2.0**	^{65}Cu(^{7}Li,t3n)	-27.8
					^{63}Cu(^{7}Li,tn)	-10.0
					^{66}Ge decay	
^{69m}Zn	13.756 h	IT (99.967)	**438.63**	**94.85 ± 0.07**	^{65}Cu(^{7}Li,^{3}He)	0.7
		β^- (0.033)			^{69}Cu decay	

^{65}Zn	243.93 d	ε+β^+ (100)	**1115.54**	**50.04 ± 0.10**	^{65}Cu(^{7}Li,α3n)	-13.1
					^{63}Cu(^{7}Li,αn)	4.7
					^{65}Ga decay	

Among the contributing reactions only the reaction with the lowest Q-value is listed.

3. Results and discussion

Direct and cumulative cross sections for formation of six radionuclides, ^{69,68}Ge, ^{67,66}Ga and ^{69m,65}Zn, were determined. The cross sections determined in the experiments #1 and #2 agree well with each other. The numerical data are summarized in Tables 4 and 5 and displayed in Figs. 1–6 in comparison with the previously published data [9] if available. Experimental physical thick target yields of the radionuclides are also summarized in Table 6 and shown in Fig. 7 in comparison with calculated ones using the experimental cross sections obtained in this work.

The total energy uncertainty was calculated from the uncertainty of the primary beam energy (±0.4 MeV) and target thicknesses (1 %). The total uncertainty of the cross section and thick target yield data was calculated from the square roots of the quadratic summation of each component; beam intensity (5 %), γ-ray intensity (0.1–11 %), detector efficiency (5 %), target thickness (1 %) and counting statistics (0.5–37 %).

Table 4. Production cross sections (mb) measured in the experiment #1.

Energy (MeV)	^{69}Ge (mb)	^{68}Ge (mb)	^{67}Ga$^{(cum)}$ (mb)	^{66}Ga$^{(cum)}$ (mb)	^{69m}Zn (mb)	^{65}Zn$^{(cum)}$ (mb)
71.0 ±0.4	1.52 ±0.27		130 ±9	106 ±10		360 ±27
68.6 ±0.4	2.00 ±0.35		142 ±10	111 ±11		378 ±28
66.0 ±0.4	2.63 ±0.43		153 ±11	120 ±11		381 ±29
63.4 ±0.4	3.09 ±0.49		161 ±12	132 ±12		386 ±29
60.7 ±0.4	4.08 ±0.62		166 ±12	151 ±14		374 ±28
57.9 ±0.4	5.28 ±0.78		166 ±12	178 ±17		359 ±27
55.0 ±0.4	6.77 ±0.97	49.8 ±9.4	162 ±12	206 ±19		320 ±24
51.9 ±0.5	9.77 ±1.36	48.3 ±10.8	159 ±12	230 ±21		277 ±21
48.8 ±0.5	14.5 ±2.0	57.1 ±11.6	165 ±12	251 ±23		231 ±17
45.4 ±0.5	20.4 ±2.8	70.2 ±13.1	183 ±13	251 ±23	1.36 ±0.31	184 ±14
41.9 ±0.6	32.9 ±4.4	66.8 ±12.2	235 ±17	237 ±22	1.71 ±0.33	147 ±11
38.2 ±0.6	52.5 ±7.0	63.6 ±11.6	318 ±23	174 ±16	2.20 ±0.32	114 ±9
34.1 ±0.7	78 ±10	41.7 ±9.3	405 ±29	104 ±10	1.99 ±0.28	98.6 ±7.6
29.7 ±0.8	100 ±13	38.3 ±8.8	451 ±33	47.3 ±4.6	1.61 ±0.24	102 ±8
24.8 ±0.9	103 ±14	48.2 ±7.3	387 ±28	21.8 ±2.2	0.756 ±0.150	118 ±9
19.1 ±1.1	66.8 ±8.9	79.7 ±11.7	193 ±14	10.6 ±1.1		136 ±10
11.9 ±1.6	7.03 ±0.97	45.1 ±5.0	16.0 ±1.2	0.412 ±0.042		60.5 ±4.5

Table 5. Production cross sections (mb) measured in the experiment #2.

Energy (MeV)	^{69}Ge (mb)	^{68}Ge (mb)	^{67}Ga$^{(cum)}$ (mb)	^{66}Ga$^{(cum)}$ (mb)	^{69m}Zn (mb)	^{65}Zn$^{(cum)}$ (mb)
70.1 ±0.4	1.74 ±0.31		140 ±10	106 ±10		354 ±27
67.5 ±0.4	2.07 ±0.36		150 ±11	112 ±11		367 ±27
65.0 ±0.4	2.49 ±0.41		161 ±12	125 ±12		389 ±29

62.3 ±0.4	3.52 ±0.54		168 ±12	139 ±13		380 ±28
59.6 ±0.4	4.44 ±0.66		172 ±13	162 ±15		363 ±27
56.7 ±0.4	5.91 ±0.86		170 ±12	188 ±17		345 ±26
53.7 ±0.5	8.86 ±1.24	53.9 ±10.6	170 ±12	227 ±21	0.606 ±0.226	310 ±23
50.7 ±0.5	12.4 ±1.7	46.3 ±10.0	169 ±12	252 ±23	1.00 ±0.33	252 ±19
47.4 ±0.5	17.8 ±2.4	54.8 ±9.8	176 ±13	261 ±24	1.21 ±0.35	204 ±15
44.0 ±0.6	28.0 ±3.8	65.8 ±11.5	217 ±16	251 ±23	1.31 ±0.27	165 ±12
40.4 ±0.6	44.4 ±5.9	64.1 ±11.3	283 ±21	205 ±19	2.02 ±0.33	126 ±10
36.6 ±0.7	66.5 ±8.9	51.9 ±9.4	379 ±28	134 ±12	1.92 ±0.28	107 ±8
32.4 ±0.7	93.5 ±12.5	40.8 ±8.2	441 ±32	64.4 ±6.2	1.78 ±0.26	94.1 ±7.3
27.8 ±0.8	107 ±14	42.6 ±9.0	437 ±32	28.1 ±2.9	0.987 ±0.193	102 ±8
22.6 ±1.0	86.8 ±11.6	60.0 ±9.9	284 ±21	15.4 ±1.8	0.394 ±0.137	127 ±10
16.4 ±1.3	26.2 ±3.5	78.3 ±11.2	63.7 ±4.7	1.89 ±0.43		107 ±8
8.1 ±2.0	0.110 ±0.039		0.148 ±0.042	0.118 ±0.015		1.71 ±0.19

Table 6. Physical thick target yields (Bq/C) measured in the experiment #3. (1 Bq/C = 0.0036 Bq/μAh)

Energy (MeV)	^{69}Ge	^{68}Ge	^{67}Ga$^{(cum)}$	^{66}Ga$^{(cum)}$	^{69m}Zn$^{(cum)}$	^{65}Zn$^{(cum)}$
71.6 ±0.4	4.9±0.7×10^{8}	4.1±0.4×10^{6}	1.8±0.1×10^{9}	9.1±0.8×10^{9}	4.0±0.5×10^{7}	2.6±0.2×10^{7}
66.2 ±0.4	4.8±0.6×10^{8}	4.4±0.5×10^{6}	1.6±0.1×10^{9}	8.2±0.8×10^{9}	3.6±0.4×10^{7}	2.1±0.2×10^{7}
60.6 ±0.4	4.7±0.6×10^{8}	3.9±0.4×10^{6}	1.5±0.1×10^{9}	7.1±0.7×10^{9}	3.4±0.4×10^{7}	1.5±0.1×10^{7}
54.4 ±0.5	4.8±0.6×10^{8}	3.4±0.4×10^{6}	1.3±0.1×10^{9}	5.5±0.5×10^{9}	3.0±0.4×10^{7}	1.1±0.1×10^{7}
47.8 ±0.5	4.5±0.6×10^{8}	2.9±0.3×10^{6}	1.1±0.1×10^{9}	3.6±0.3×10^{9}	2.5±0.3×10^{7}	6.6±0.5×10^{6}
40.4 ±0.7	4.0±0.5×10^{8}	1.8±0.2×10^{6}	9.0±0.7×10^{8}	1.5±0.1×10^{9}	2.0±0.3×10^{7}	4.2±0.3×10^{6}
31.9 ±0.8	2.7±0.4×10^{8}	1.3±0.2×10^{6}	5.2±0.4×10^{8}	2.8±0.3×10^{8}	1.0±0.3×10^{7}	2.7±0.2×10^{6}
21.5 ±1.2	5.8±0.8×10^{7}	6.3±1.2×10^{5}	8.3±0.6×10^{7}	3.1±0.6×10^{7}		1.1±0.1×10^{6}

3.1 ^{69}Ge production

The production cross sections of ^{69}Ge ($T_{1/2}$ = 39.05 h) were determined using the γ line at 1106.77 keV (I_γ = 36 %) emitted in its decay. The possible interference γ line at 1106.53 keV from ^{66}Ga ($T_{1/2}$ = 9.49 h) was negligible because of its very low intensity (I_γ = 0.0012 %) and the applied long cooling time. The spectra measured in Ser. 3 (average cooling time ~4 d) were used to determine the cross sections.

The derived cross sections are shown in Fig. 1 with the previously published data [9]. Our results in the two experiments (#1 and #2) agree with the previously published data except a slight deviation at the lower energy region. The excitation function of the reaction shows a smooth curve and a peak at around 30 MeV. The reaction has relatively low threshold energy and more than 100 mb cross section values at maximum. These features are appropriate for using the ^{nat}Cu(^{7}Li,x)^{69}Ge reaction as a monitor reaction. However, the uncertainty of the γ line is relatively large (11 %). This reaction can be used as a monitor reaction after the γ-ray intensity is determined more precisely.

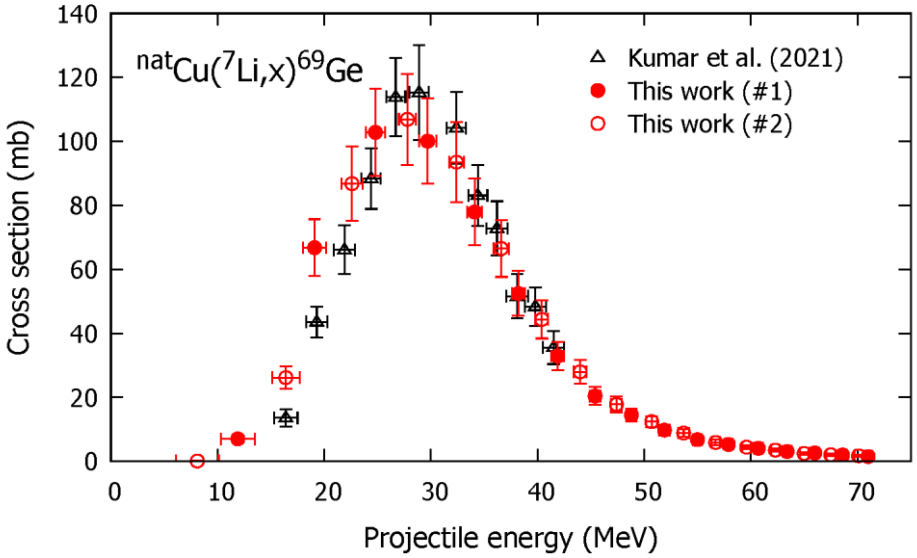


Fig. 1. Cross sections of the ^{nat}Cu(^{7}Li,x)^{69}Ge reaction in comparison with the previously published data [9].

3.2 ^{68}Ge production

Cross sections of the ^{nat}Cu(^{7}Li,x)^{68}Ge reaction were measured. There are no γ lines emitted from the decay of ^{68}Ge ($T_{1/2}$ = 270.93 d). The γ line at 1077.34 keV (I_γ = 3.22 %) from the daughter nucleus ^{68}Ga ($T_{1/2}$ = 67.71 min) in equilibrium was used for its quantification. The same γ lines emitted from ^{68}Cu ($T_{1/2}$ = 30.9 s) and ^{68m}Cu ($T_{1/2}$ = 3.75 min) could be neglected because of their short half-lives. The spectra measured in Ser. 4 were used to determine the cross sections.

The derived cross sections of the reaction are shown in Fig. 2. No previously published data were found for this reaction. The statistical uncertainty is relatively large (8.3–22 %) due to the low γ-ray intensity and long half-life. The excitation function shows two local maxima corresponding to contributions from the ^{63}Cu(^{7}Li,2n)^{68}Ge and ^{65}Cu(^{7}Li,4n) ^{68}Ge reactions. Due to the low γ-ray intensity and long half-life of ^{68}Ge this reaction requires long γ-ray measurements for reducing the statistical uncertainty. Thus, this reaction can be used as a monitor reaction when long γ-ray measurements are possible to carry out.

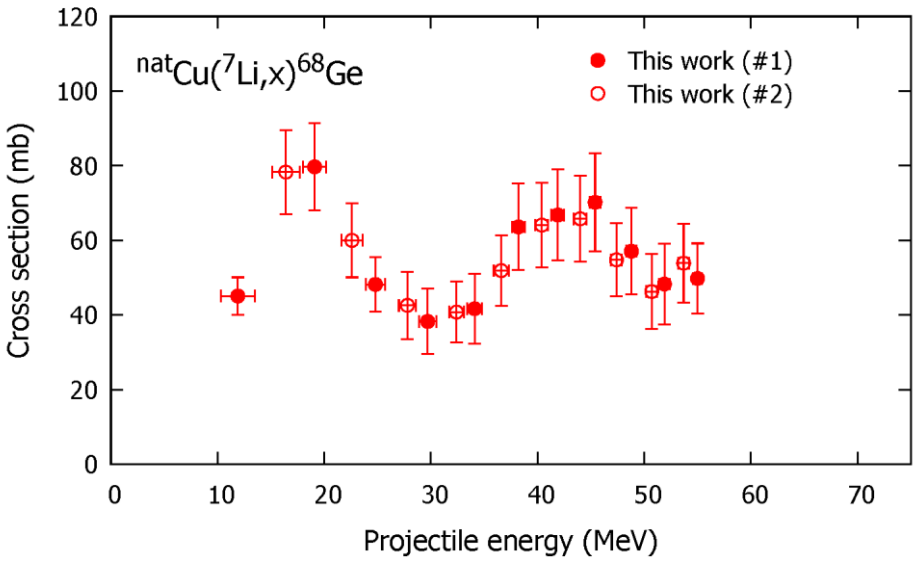


Fig. 2. Cross sections of the ^{nat}Cu(^{7}Li,x)^{68}Ge reaction.

3.3 ^{67}Ga production

Cumulative cross sections can be deduced for formation of ^{67}Ga ($T_{1/2}$ = 3.2617 d). This radionuclide can be produced directly in several possible reactions and also in decay of ^{67}Ge ($T_{1/2}$ = 18.9 min). There are three intense γ lines at 93.31 (I_γ = 38.81 %), 184.58 (I_γ = 21.410 %) and 300.22 keV (I_γ = 16.64 %) from the decay of ^{67}Ga that is used in data analyses. However, as ^{67}Cu ($T_{1/2}$ = 61.83 h) is also co-produced and generates interference for all the three γ lines with different intensities (I_γ = 16.1 %, 48 % and 0.797 %, respectively). Among them the γ line at 300.22 keV was selected to determine the excitation function in order to reduce the possible interference. In order to estimate the effect of the ^{67}Cu contribution, the cross sections were also calculated using the E_γ = 184.58 keV, the highest intensity γ line of ^{67}Cu. The deduced cross sections were for 5.2 % higher than the ones deduced using the 300.22-keV γ line. Considering the ratio of the γ-ray intensities the ^{67}Cu contribution to the 300.22-keV γ line was estimated and found to be less than 0.1 % and therefore was neglected. The spectra measured in Ser. 4 were used to determine the cross sections. The parent nucleus ^{67}Ge decayed completely during the long cooling time.

The cumulative formation cross sections of ^{67}Ga are shown in Fig. 3 with the previously published data [9]. The peak position and amplitude of the previously published data are different from our data. The excitation function of the ^{nat}Cu(^{7}Li,x)^{67}Ga reaction is smoothly changed and has a peak at around 30 MeV. This reaction is expected to be a monitor reaction using the 300.22-keV γ line for the ^{67}Ga activity calculation.

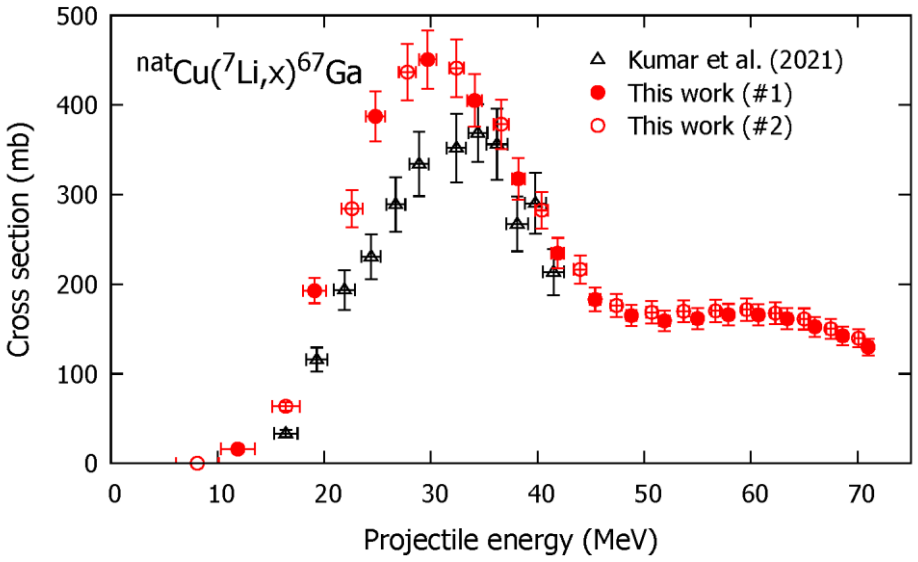


Fig. 3. Cumulative cross sections of the ^{nat}Cu(^{7}Li,x)^{67}Ga reaction with the previously published data [9].

3.4 ^{66}Ga production

Several direct reactions can contribute to the production of ^{66}Ga ($T_{1/2}$ = 9.49 h). Production through the decay of ^{66}Ge ($T_{1/2}$ = 2.26 h) is also possible above 23.6 MeV. The 1039.22-keV γ line (I_γ = 37.0 %) was used to determine production cross sections of ^{66}Ga. The contribution from decay of the shorter-lived nucleus ^{66}Cu ($T_{1/2}$ = 5.120 min) to the same γ line was negligible in the spectra in Ser. 2 with the cooling time longer than 5.2 h. The parent nuclide ^{66}Ge was produced in negligible amount, because its intense γ line with energy of 381.85 keV (I_γ = 28.3 %) was missing in the spectra. Another isotope ^{70}Ga ($T_{1/2}$ = 21.14 min) may contribute to the 1039.2-keV γ line, but due to its short half-life and low γ-ray intensity (I_γ = 0.65 %) its contribution was also neglected.

The derived cumulative cross sections are shown in Fig. 4 with the previously published data [9]. The previously published data are smaller than our data. The excitation function of the ^{nat}Cu(^{7}Li,x)^{66}Ga reaction has suitable shape and sufficiently high cross sections for being used for the beam monitoring.

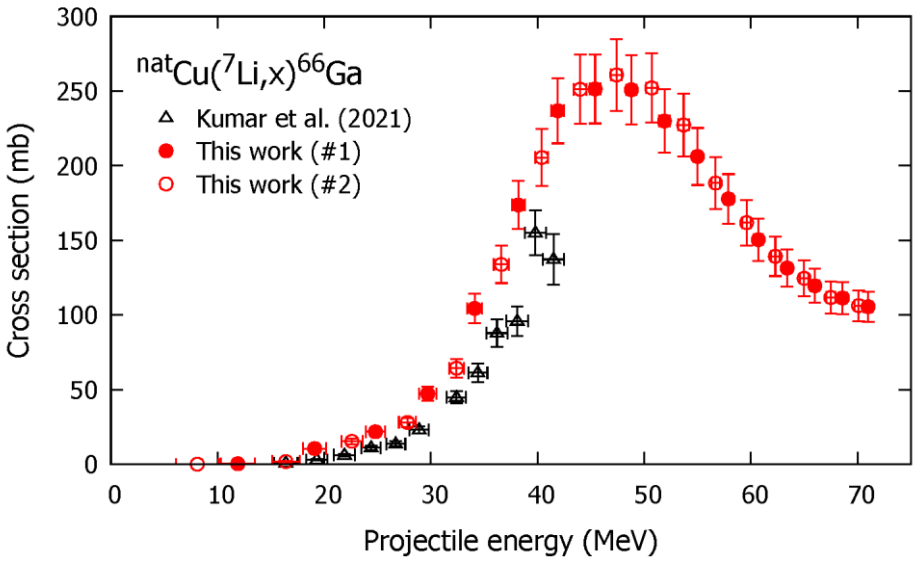


Fig. 4. Cumulative cross sections of the ^{nat}Cu(^{7}Li,x)^{66}Ga reaction with the previously published data [9].

3.5 ^{69m}Zn production

Among the two stable isotopes of copper, only ^{65}Cu can contribute to the production of ^{69m}Zn ($T_{1/2}$ = 13.756 h). The strong and interference-free γ line at 438.63 keV (I_γ = 94.85 %) was used to derive the production cross sections of ^{69m}Zn. The short-lived parent nucleus ^{69}Cu ($T_{1/2}$ = 2.85 min) decayed to the ground state ^{69g}Zn soon after the end-of-bombardment and do not populate the excited state ^{69m}Zn. The spectra in Ser. 2 were used to determine the cross sections.

The deduced cross sections are shown in Fig. 5 with the previously published data [9]. The peak position of the previously published data is consistent with ours although the amplitude is slightly smaller. The statistical uncertainty is large (12–37 %) because the cross sections are much smaller than those of Ge and Ga radionuclides in sections 3.1–3.4. The reaction does not seem, therefore, to be suitable for the beam monitoring purposes.

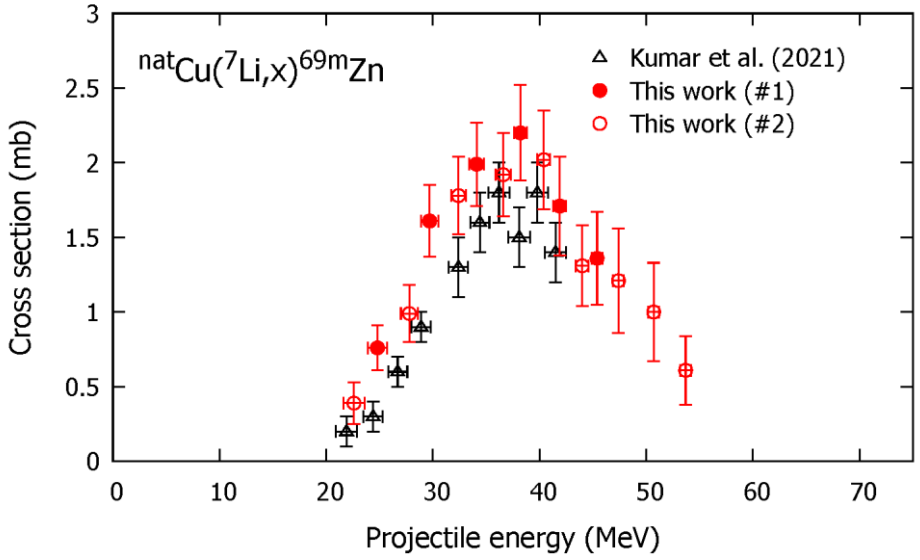


Fig. 5. Cross sections of the ^{nat}Cu(^{7}Li,x)^{69m}Zn reaction with the previously published data [9].

3.6 ^{65}Zn production

The intense and interference-free γ line at 1115.54 keV (I_γ = 50.04 %) was used to determine the production cross sections of ^{65}Zn ($T_{1/2}$ = 243.93 d). The two parent nuclei ^{65}Ge ($T_{1/2}$ = 30.9 s) and ^{65}Ga ($T_{1/2}$ = 15.2 min) decayed during the cooling time of Ser. 4. The possible interference from decay of ^{65}Ni ($T_{1/2}$ = 2.52 h) was also eliminated during the long cooling time.

Determination of the cumulative cross sections was straightforward. The results are shown in Fig. 6 in comparison with the previously published data [9]. The previously published data are again somewhat smaller than ours. The excitation function from the present work is changing smoothly in terms of the projectile energy and has two peaks at around 20 and 65 MeV. The cross sections are high up to almost 400 mb. Considering the course and amplitudes of this reaction, it can be suggested as a monitor reaction.

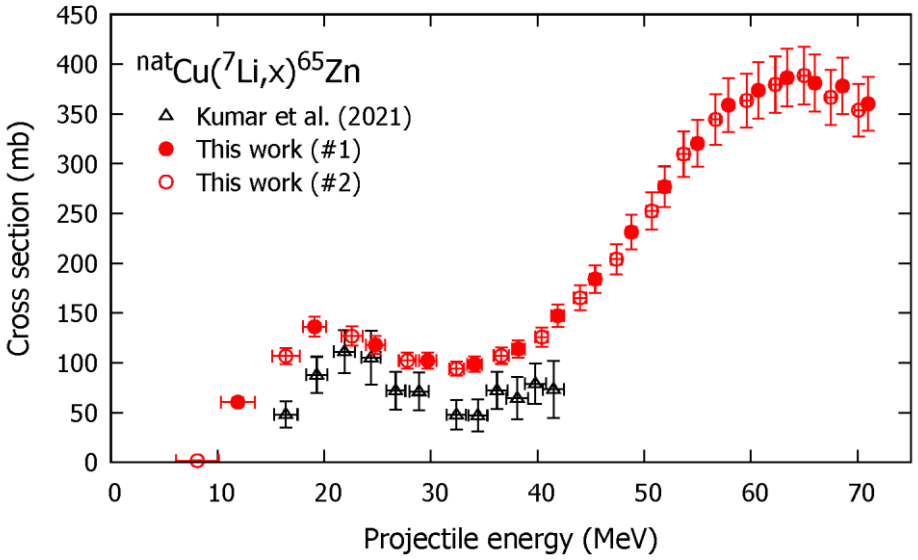


Fig. 6. Cumulative cross sections of the ^{nat}Cu(^{7}Li,x)^{65}Zn reaction with the previously published data [9].

3.7 Physical thick target yields

Physical thick target yields [15] of ^{69,68}Ge, ^{67,66}Ga and ^{69m,65}Zn were experimentally determined using Eq. (2) to assess the measured cross sections. The stack of 8 Cu foils (25-μm thick each) was irradiated. The 200-μm thick stack was able to stop the incident ^{7}Li beam. By measuring the activity of the eight foils separately it was possible to build up the energy dependent thick target yield curves for the investigated reactions. In the γ-ray measurements recoil and self-attenuation effects were neglected. The amounts of recoiled reaction products were expected to be much smaller than those remaining in the foils because of the foil thickness (25-μm thick). The self-attenuation for the lowest γ-ray energy in the measurements (E_γ = 300.22 keV) by one Cu foil was estimated using the mass attenuation coefficient [16] and found to be less than 0.2 %. The maximum γ-ray attenuation by seven Cu foils for the γ rays was estimated to be less than 1.7 %. The attenuation was affected by the distribution of products in the target foils and neglected. To determine the activity of the produced different radionuclides the same γ lines were used for the cross section measurements.

The experimentally determined physical thick target yields (symbols) are shown in Fig. 7 in comparison with calculated ones (lines) using Eq. (3) with the experimental cross section data determined in this work. The corresponding results are in good agreement with each other. The proper agreements between the measured and calculated yields increase the reliability of both the deduced cross sections and the experimental yields in this work.

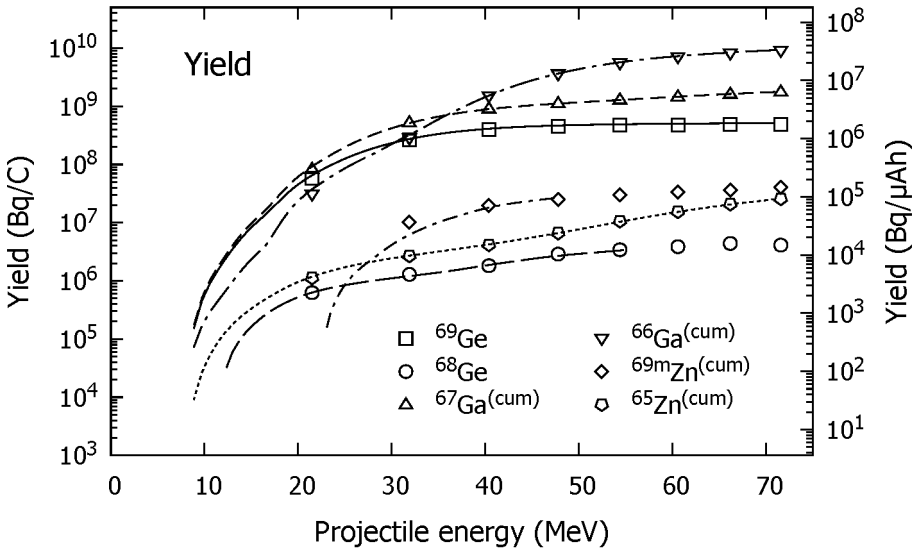


Fig. 7. Experimental physical thick target yields of ^{69,68}Ge, ^{67,66}Ga and ^{69m,65}Zn in comparison with those derived from the cross sections measured in this work. (1 Bq/C = 0.0036 Bq/μAh)

4. Conclusion

Activation cross sections and physical thick target yields of the ^{7}Li-induced reactions on ^{nat}Cu were determined. Production cross sections of ^{69,68}Ge, ^{67,66}Ga and ^{69m,65}Zn were measured and compared with the available experimental data. In most cases, the previously published data are lower than our results. For benchmarking physical thick target yields were also determined and compared with the calculated values based on the experimental cross sections measured in this work. Good agreements are found between the measured and calculated yield data for every reaction. This agreement confirms reliability of both the cross sections and thick target yield data. As suggested by the obtained data, the reactions resulting in ^{67,66}Ga and in ^{65}Zn are potential beam monitors for ^{7}Li.

Acknowledgment

This work was carried out at RI Beam Factory operated by RIKEN Nishina Center and CNS, University of Tokyo, Japan. The authors would like to thank Dr. Y. Shigekawa, Dr. Y. Kanayama, and Mr. A. Nambu of RIKEN Nishina Center for technical assistance with the experiment. DI would like to show the gratitude for the support by Mongolian Foundation for Science and Technology under the grant number 2022/159.

Declarations of interest

None.

Reference

[1] M. R. Zalutsky, M. Pruszynski, Astatine-211: Production and Availability, Curr Radiopharm 4 (2011) 177–185. https://doi.org/10.2174/1874471011104030177.

[2] A. Morgenstern, K. Abbas, F. Bruchertseifer, C. Apostolidis, Production of Alpha Emitters for Targeted Alpha Therapy, Curr Radiopharm 1 (2008) 135–143. https://doi.org/10.2174/1874471010801030135.

[3] F. Guérard, J.F. Gestin, M.W. Brechbiel, Production of [211At]-astatinated radiopharmaceuticals and applications in targeted α-particle therapy, Cancer Biother Radiopharm 28 (2013) 1–20. https://doi.org/10.1089/cbr.2012.1292.

[4] G.J. Meyer, R.M. Lambrecht, Excitation function for the ^{209}Bi(^{7}Li, 5n)^{211}Rn nuclear reaction, Int J Appl Radiat Isot 31 (1980) 351–355. https://doi.org/10.1016/0020-708X(80)90125-8.

[5] E. Maeda, A. Yokoyama, T. Taniguchi, K. Washiyama, I. Nishinaka, Measurements of the excitation functions of radon and astatine isotopes from ^{7}Li-induced reactions with ^{209}Bi for development of a ^{211}Rn–^{211}At generator, J Radioanal Nucl Chem 323 (2020) 921–926. https://doi.org/10.1007/s10967-019-06990-z.

[6] A. Hermanne, A. V. Ignatyuk, R. Capote, B. V. Carlson, J.W. Engle, M.A. Kellett, T. Kibédi, G. Kim, F.G. Kondev, M. Hussain, O. Lebeda, A. Luca, Y. Nagai, H. Naik, A.L. Nichols, F.M. Nortier, S. V. Suryanarayana, S. Takács, F.T. Tárkányi, M. Verpelli, Reference Cross Sections for Charged-particle Monitor Reactions, Nuclear Data Sheets 148 (2018) 338–382. https://doi.org/10.1016/j.nds.2018.02.009.

[7] F. Tárkányi, S. Takács, K. Gul, A. Hermanne, M.G. Mustafa, M. Nortier, P. Obložinský, S.M. Qaim, B. Scholten, Yu.N. Shubin, Z. Yousiang, Beam monitor reactions, in: Charged Particle Cross-Section Database for Medical Radioisotope Production, IAEA-TECDOC-1211, 2001.

[8] N. Otuka, E. Dupont, V. Semkova, B. Pritychenko, A.I. Blokhin, M. Aikawa, S. Babykina, M. Bossant, G. Chen, S. Dunaeva, R.A. Forrest, T. Fukahori, N. Furutachi, S. Ganesan, Z. Ge, O.O. Gritzay, M. Herman, S. Hlavač, K. Kato, B. Lalremruata, Y.O. Lee, A. Makinaga, K. Matsumoto, M. Mikhaylyukova, G. Pikulina, V.G. Pronyaev, A. Saxena, O. Schwerer, S.P. Simakov, N. Soppera, R. Suzuki, S. Takács, X. Tao, S. Taova, F. Tárkányi, V. V. Varlamov, J. Wang, S.C. Yang, V. Zerkin, Y. Zhuang, Towards a More complete and accurate experimental nuclear reaction data library (EXFOR): International collaboration between nuclear reaction data centres (NRDC), Nuclear Data Sheets 120 (2014) 272–276. https://doi.org/10.1016/j.nds.2014.07.065.

[9] R. Kumar, M. Maiti, T.N. Nag, S. Sodaye, Exploring various features of the reaction mechanism involved in the collision of ^{7}Li on Cu, Phys Rev C 104 (2021) 064606. https://doi.org/10.1103/PhysRevC.104.064606.

[10] T. Watanabe, M. Fujimaki, N. Fukunishi, H. Imao, O. Kamigaito, M. Kase, M. Komiyama, N. Sakamoto, K. Suda, M. Wakasugi, K. Yamada, Beam energy and longitudinal beam profile measurement system at the RIBF, in: Proceedings of the 5th International Particle Accelerator Conference (IPAC 2014), 2014: pp. 3566–3568.

[11] J.F. Ziegler, J.P. Biersack, M.D. Ziegler, SRIM: the Stopping and Range of Ions in Matter, (2008). http://www.srim.org.

[12] National Nuclear Data Center, Nuclear structure and decay data on-line library, Nudat 3.0, (2021). http://www.nndc.bnl.gov/nudat3/.

[13] International Atomic Energy Agency, LiveChart of Nuclides, (2009). https://www-nds.iaea.org/livechart/.

[14] B. Pritychenko, A. Sonzogni, Q-value Calculator (QCalc), (2003). http://www.nndc.bnl.gov/qcalc/.

[15] N. Otuka, S. Takács, Definitions of radioisotope thick target yields, Radiochim Acta 103 (2015) 1–6. https://doi.org/10.1515/ract-2013-2234.

[16] J.H. Hubbel, S.M. Seltzer, X-Ray Mass Extinction Coefficients, NIST Standard Reference Database 126 (2004). https://doi.org/https://doi.org/10.18434/T4D01F.